blood®
Regular Article

Check for updates

LYMPHOID NEOPLASIA

A MIR17HG-derived long noncoding RNA provides an essential chromatin scaffold for protein interaction and myeloma growth

Eugenio Morelli,[1,2] Mariateresa Fulciniti,[1,2] Mehmet K. Samur,[1,2] Caroline F. Ribeiro,[3] Leon Wert-Lamas,[4] Jon E. Henninger,[5] Annamaria Gullà,[1,2] Anil Aktas-Samur,[1,2] Katia Todoerti,[6] Srikanth Talluri,[1,2,7] Woojun D. Park,[8] Cinzia Federico,[9] Francesca Scionti,[9,10] Nicola Amodio,[9] Giada Bianchi,[1,2] Megan Johnstone,[1] Na Liu,[1] Doriana Gramegna,[1,2] Domenico Maisano,[1,2] Nicola A. Russo,[11] Charles Lin,[8] Yu-Tzu Tai,[1,2] Antonino Neri,[6,12,13] Dharminder Chauhan,[1,2] Teru Hideshima,[1,2] Masood A. Shammas,[1,2,7] Pierfrancesco Tassone,[9] Sergei Gryaznov,[14] Richard A. Young,[5] Kenneth C. Anderson,[1,2] Carl D. Novina,[4] Massimo Loda,[3] and Nikhil C. Munshi[1,2,7]

[1]Department of Medical Oncology, Jerome Lipper Multiple Myeloma Center, Dana-Farber Cancer Institute, Boston, MA; [2]Harvard Medical School, Boston, MA; [3]Department of Pathology and Laboratory Medicine, Weill Cornell Medical College, New York, NY; [4]Department of Cancer Immunology and Virology, Dana-Farber Cancer Institute, Boston, MA; [5]Whitehead Institute of Biomedical Research, Massachusetts Institute of Technology, Cambridge, MA; [6]Department of Hematology, Fondazione Cà Granda IRCCS Policlinico, Milan, Italy; [7]VA Boston Healthcare System, Boston, MA; [8]Department of Molecular and Human Genetics, Baylor College of Medicine, Houston, TX; [9]Department of Clinical and Experimental Medicine, Magna Graecia University, Catanzaro, Italy; [10]Clinical Research Development and Phase I Unit, ASST Spedali Civili di Brescia, Brescia, Italy; [11]Istituto di Ricerche Genetiche "G. Salvatore," Biogem s.c.ar.l., Avellino, Italy; [12]Department of Oncology and Hemato-oncology, University of Milan, Milan, Italy; [13]Scientific Directorate, Azienda USL-IRCCS Reggio Emilia, Reggio Emilia, Italy; and [14]Maia Biotechnology Inc, Chicago, IL

KEY POINTS

- **MIR17HG produces a long noncoding RNA that acts as a chromatin scaffold for protein interaction and tumor cell growth.**
- **Targeting this long noncoding RNA with optimized antisense oligonucleotides has potent antimyeloma activity in preclinical models.**

Long noncoding RNAs (lncRNAs) can drive tumorigenesis and are susceptible to therapeutic intervention. Here, we used a large-scale CRISPR *interference* viability screen to interrogate cell-growth dependency to lncRNA genes in multiple myeloma (MM) and identified a prominent role for the *miR-17-92 cluster host gene* (*MIR17HG*). We show that an *MIR17HG*-derived lncRNA, named lnc-17-92, is the main mediator of cell-growth dependency acting in a microRNA- and DROSHA-independent manner. Lnc-17-92 provides a chromatin scaffold for the functional interaction between c-MYC and WDR82, thus promoting the expression of *ACACA*, which encodes the rate-limiting enzyme of de novo lipogenesis acetyl-coA carboxylase 1. Targeting *MIR17HG* pre-RNA with clinically applicable antisense molecules disrupts the transcriptional and functional activities of lnc-17-92, causing potent antitumor effects both in vitro and in vivo in 3 preclinical animal models, including a clinically relevant patient-derived xenograft NSG mouse model. This study establishes a novel oncogenic function of *MIR17HG* and provides potent inhibitors for translation to clinical trials.

Introduction

Multiple myeloma (MM) is a genetically complex malignancy of plasma cells that accounts for ~10% of hematologic cancers and remains largely incurable.[1] A growing body of evidence points to a key role played by noncoding RNA (ncRNA) networks in MM,[2] suggesting that MM cells can become significantly addicted to and therapeutically susceptible to the modulation of oncogenic ncRNAs.[3-8] In particular, long ncRNAs (lncRNAs) outnumber protein-coding genes in humans and are susceptible to the same oncogenic pathogenetic events.[9,10] These RNA molecules, defined as transcripts greater than 200 nucleotides (nt) with no protein-coding potential, have a diverse array of functional roles, ranging from being precursor molecules for the biogenesis of mature microRNAs (miRNAs) to direct interactions with proteins and nucleic acids to regulate protein function and/or stability.[11-13] With the plethora of biological functions that lncRNAs modulate to control cellular processes at multiple levels, it is not surprising that their aberrant expression and function have been implicated in the progressive gain of a malignant phenotype by tumor cells.[14] Indeed, the expression of 14 lncRNAs in newly diagnosed MM patients is correlated (or anticorrelated) with progression-free survival independent of cytogenetic, international staging system, or minimal residual disease status.[15] Other lncRNAs, including SMILO, also independently predict MM progression and response to therapy.[16,17]

To find lncRNAs that have a direct impact on MM proliferation and survival, thus providing cell-growth dependency, we conducted an lncRNA-targeted large-scale CRISPR *interference*

Downloaded from http://ashpublications.org/blood/article-pdf/141/4/391/2031172/blood_bld-2022-016892-main.pdf by guest on 30 June 2023

(CRISPRi) viability screen. CRISPRi makes use of a catalytically inactive Cas9 (dCas9)-KRAB fusion protein to repress the expression of endogenous lncRNA genes.[18,19] From this screen, we identified *MIR17HG* as essential in MM, and we (1) characterized its novel function as lncRNA mediating protein-protein and protein-DNA interactions and (2) developed potent inhibitors for translation to clinical trials.

Methods

Cells

Human cell lines and primary cells were grown at 37°C, 5% CO_2. Detailed information is included in supplemental Methods, available on the *Blood* website.

RNA sequencing, microarray-based gene expression analysis, and miRNA profiling of MM patients and cell lines

These analyses were performed in purified $CD138^+$ cells. Detailed information can be found in supplemental Methods.

CRISPRi viability screen and validation

Cell lines expressing the dCas9-KRAB fusion protein were generated as previously described.[19] Detailed information on library design, guide RNA pool library production, titering of virus, primary and secondary screenings, and validation study as well as on data analysis can be found in supplemental Methods.

ASO, synthetic miRNA mimics and inhibitors, siRNAs

Long noncoding locked nucleic acid gapmeRs were custom designed and purchased from Exiqon (Vedbaek, Denmark). Sequences can be found in supplemental Methods. Synthetic miRNA mimics and inhibitors, as well as silencer select small interfering RNAs (siRNAs), were purchased from Ambion. SiRNA pool targeting WDR82 was purchased from Horizon Discovery. Design of clinically applicable antisense oligonucleotides (ASOs) is described in supplemental Table 8.

Gymnosis

Gymnotic experiments were performed as previously described.[20]

Transient and stable transfection of cells

Cell transfection and transduction were performed as previously described.[5] Detailed information can be found in supplemental Methods.

Detection of cell proliferation and apoptosis

Cell viability was evaluated by Cell Counting Kit-8 (CCK-8) assay (Dojindo Molecular Technologies), according to the manufacturer's instructions. Apoptosis was investigated by an Annexin V/7-AAD flow cytometry assay using FACS CANTO II (BD Biosciences).

RT and qRT-PCR

RNA extraction, reverse transcription (RT), and real-time quantitative reverse transcription polymerase chain reaction (qRT-PCR) were performed as previously described.[5] Detailed information can be found in supplemental Methods.

Western blot analysis

Protein extraction and Western blot analysis were performed as previously described. Detailed information can be found in supplemental Methods.

RNA fluorescence in situ hybridization and coimmunofluorescence with RNA fluorescence in situ hybridization

These experiments were conducted according to established protocols.[21,22] Detailed information can be found in supplemental Methods.

Luciferase reporter assay

Promoter reporter clones for human *ACACA* (NM_198834), *ANO6* (NM_001025356), *CCDC91* (NM_018318), *EPT1* (NM_033505), *EXT1* (NM_000127), *FER* (NM_001308028), and *ZYG11A* (NM_001004339) were cloned into the GLuc-ON Promoter Reporter Vector (GeneCopoeia, Rockville, MD). A luciferase reporter assay was performed according to the manufacturer's instructions.

ChIRP

Lnc-17-92 and LacZ antisense DNA probes were designed using the online probe designer at singlemoleculefish.com. Oligonucleotides were biotinylated at the 3′ end with an 18-carbon spacer arm. AMO1 cells were collected and subjected to chromatin isolation by RNA precipitation (ChIRP) using the EZ-Magna ChIRP RNA Interactome Kit (Millipore Sigma, Bedford, MA), according to the manufacturer's instructions and established protocols.[23]

De novo lipogenesis assay

These experiments were conducted as previously described.[24] Detailed information can be found in supplemental Methods.

Chromatin immunoprecipitation quantitative polymerase chain reaction

Chromatin immunoprecipitation quantitative polymerase chain reaction was performed as previously described.[25] Detailed information can be found in supplemental Methods.

RNA-protein pull-down

Lnc-17-92 transcripts and truncated versions were cloned into a pBlueScript vector and sequence verified. In vitro transcription and biotinylation were performed using AmpliScribe T7-Flash Biotin-RNA Transcription Kit (Lucigen, catalog no. ASB71110), according to the manufacturer's instructions. Cell nuclear lysates (from 1×10^7 AMO1 cells) were incubated with biotinylated RNA and streptavidin beads for RNA pull-down incubation, using Pierce Magnetic RNA-Protein Pull-Down Kit (Thermo Fisher Scientific, catalog no. 20164), according to the manufacturer's instructions. RNA-associated proteins were eluted and analyzed by Western blotting.

RNA yeast 3 hybrid

These experiments were conducted according to established protocols.[21,22] Detailed information can be found in supplemental Methods.

Downloaded from http://ashpublications.org/blood/article-pdf/141/4/391/2031172/blood_bld-2022-016892-main.pdf by guest on 30 June 2023

RIP quantitative polymerase chain reaction

RNA immunoprecipitation (RIP) experiments were performed using the Magna RIP RNA-binding Protein Immunoprecipitation Kit (Millipore Sigma, catalog no. 17-701), according to the manufacturer's instructions. The anti-MYC antibody used for RIP was purchased from Abcam (ab32072). Normal rabbit immunoglobulin G was purchased from Cell Signaling Technology (catalog no. 2729). The primers used for detecting lnc-17-92 are listed in supplemental Methods.

Co-IP

Protein lysates were obtained from 1 × 10^7 cells (AMO1, H929, and U266^{MYC+}, with corresponding treatments). Coimmunoprecipitation (Co-IP) was performed using the Pierce Co-Immunoprecipitation Kit (Thermo Fisher Scientific, catalog no. 26149), according to the manufacturer's instructions. IP antibodies are listed in supplemental Methods.

BioID

Proximity-dependent biotin identification (BioID) was performed as described by Kalkat et al.[26] Detailed information can be found in supplemental Methods.

Mass spectrometry

Mass spectrometry analysis of Co-IP and BioID samples was performed at the Taplin Mass Spectrometry Facility (Harvard Medical School, Boston, MA).

Animal study

Six-week-old female immunodeficient NOD.CB17-Prkdcscid/NCrCrl (NOD/SCID) mice (Charles River) or NSG mice (Jackson Laboratory) were housed in our animal facility at the Dana-Farber Cancer Institute (DFCI). All experiments were performed after approval by the Animal Ethics Committee of the DFCI and performed using institutional guidelines. Detailed information can be found in supplemental Methods.

Statistical analysis

All in vitro experiments were repeated at least 3 times and performed in triplicate. Statistical significances of differences were determined using the Student *t* test (unless otherwise specified), with the minimal level of significance specified as $P < .05$. Kaplan-Meier survival curves were compared by log-rank test. Statistical analyses were determined using GraphPad software (http://www.graphpad.com). Graphs were obtained using GraphPad software (unless otherwise specified).

Results

CRISPRi viability screens identify *MIR17HG* as a leading cell-growth dependency in MM

We analyzed RNA sequencing (RNA-seq) data from 360 newly diagnosed MM patients and identified 913 lncRNA transcripts expressed in primary MM cells (Figure 1Ai.) and in a panel of 70 MM cell lines (data not shown). To systematically interrogate the role of these lncRNAs in MM cell growth, we transduced 3 MM cell lines (H929, KMS-11, and KMS-12-BM) engineered to express a dCas9-KRAB fusion protein with a pooled library consisting of 7 single guide RNAs (sgRNAs) against each of the 913 transcription start sites (TSS) of the identified lncRNAs and 576 negative control sgRNAs (Figure 1Aii; supplemental Table 1). After 3 weeks, we tested for sgRNAs that were relatively depleted or enriched in the MM cell population using deep sequencing and the Model-based Analysis of Genome-wide CRISPR-Cas9 Knockout RRA algorithm.[27]

The most enriched or depleted sgRNAs were further tested in secondary screens using a pooled library targeting the TSS of 224 lncRNAs, the TSS of known protein-coding oncogenes (MYC, IRF4),[28,29] or tumor suppressors (TP53)[30] as positive controls and 2245 nontargeting sgRNAs as negative controls (Figure 1Aiii; supplemental Table 2). In the secondary screens, 4 MM cell lines (H929, KMS11, KMS12BM, and AMO1) were used to detect and rank significantly depleted or enriched sgRNAs. As expected, sgRNAs targeting IRF4 and MYC were significantly depleted in 3 (MYC) or all (IRF4) cell lines, whereas sgRNAs targeting TP53 were significantly enriched in both TP53 wild-type (WT) cell lines (AMO1 and H929).[31]

Focusing on depleted sgRNAs, we identified lncRNA dependencies in MM cells that were either cell-line specific (54%) or shared (46%) (supplemental Figure 1A; supplemental Table 3). A ranked analysis of sgRNA depletion identified *MIR17HG* as the leading dependency, with RRA scores equal or superior to those obtained by targeting MYC or IRF4 in all cell lines tested (Figure 1B). To validate this data further, we next transduced MM cell lines expressing dCas9-KRAB fusion protein with the top 4 sgRNAs targeting *MIR17HG* under the regulation of a tetracycline-inducible promoter and observed reduced cell growth compared with cells infected with nontargeting sgRNAs after continued exposure to doxycycline (Figure 1C; supplemental Figure 1B). Moreover, we used 2 different locked nucleic acid gapmeR ASOs (simply referred to as ASO), which target the *MIR17HG* nascent RNA (pre-RNA) for ribonuclease (RNase) H–mediated degradation,[32,33] to transfect 11 MM cell lines including those resistant to conventional anti-MM agents (AMO1-ABZB resistant to bortezomib; AMO1-ACFZ resistant to carfilzomib; MM.1R resistant to dexamethasone) and confirmed a significant impact on MM cell viability independent of the genetic and molecular background (Figure 1D; supplemental Figure 1C).

MIR17HG-derived lnc-17-92 mediates cell-growth dependency in an miRNA- and DROSHA-independent manner

MIR17HG is the locus of the miRNA cluster miR-17-92 and an lncRNA,[34,35] named here lnc-17-92. Lnc-17-92 has 2 isoforms, 1 that is ~5000 nt long (lnc-17-92^{TV1}) and 1 that is ~900 nt (lnc-17-92^{TV2}),[34,35] and both have yet to be functionally explored (Figure 2A). In MM cells, both RNA-seq (supplemental Figure 2A) and qRT-PCR (supplemental Figure 2B) indicated preferential expression of lnc-17-92^{TV1}, which is the isoform further investigated in this study and hereafter referred to as lnc-17-92. Using RNA-seq, we confirmed its expression in CD138$^+$ cells from an additional large cohort of MM patients (MMRF/CoMMpass, n = 720) and in MM cell lines (n =60) (supplemental Figure 2C-D). In MM cell lines, we also demonstrated nuclear enrichment of lnc-17-92 using single molecule RNA fluorescence in situ hybridization (FISH) (Figure 2B) and subcellular qRT-PCR (supplemental Figure 2E). We observed that lnc-17-92 expression was higher during disease progression in 2 independent data sets from MM patients analyzed at

Downloaded from http://ashpublications.org/blood/article-pdf/141/4/391/2031172/blood_bld-2022-016892-main.pdf by guest on 30 June 2023

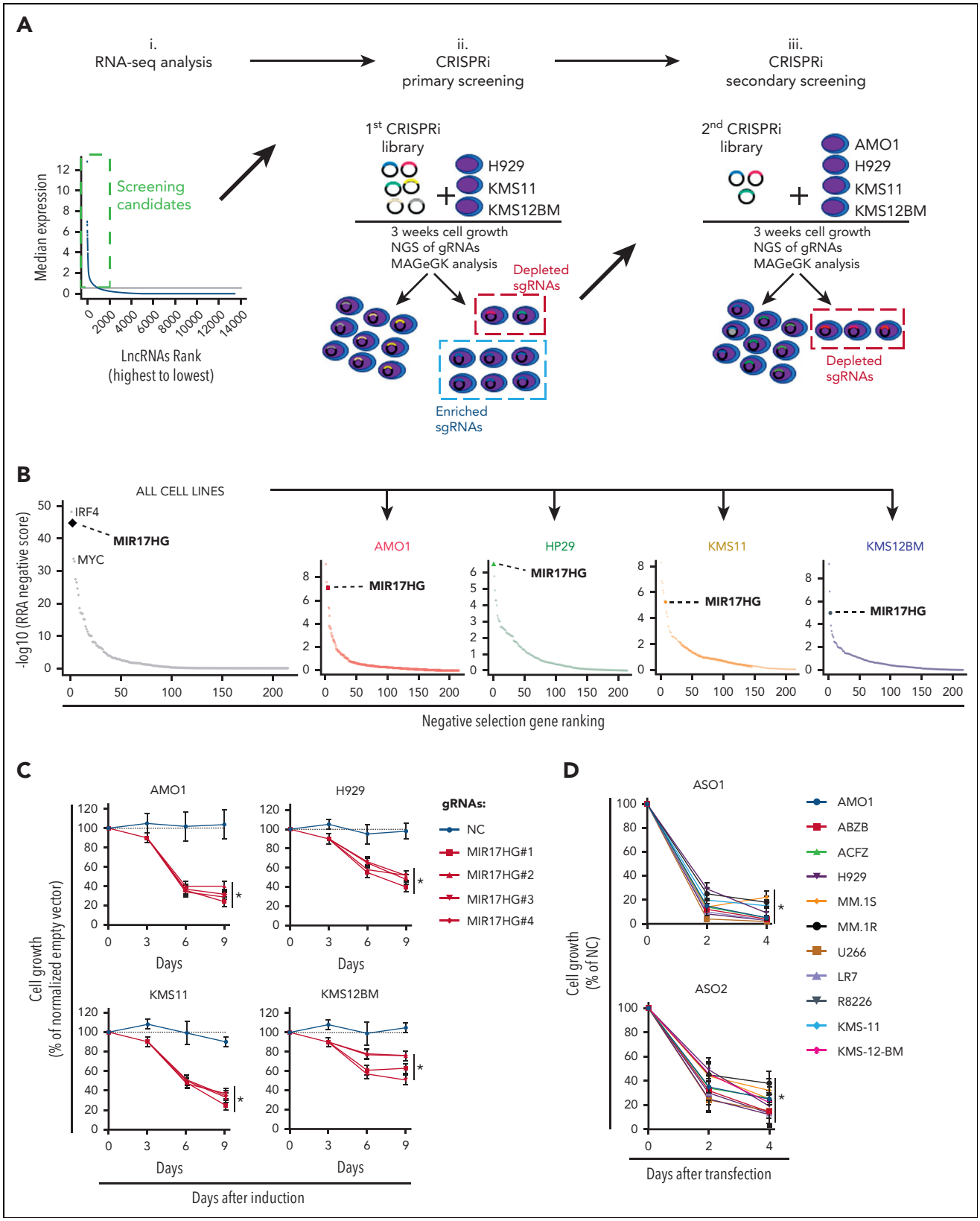

Figure 1. CRISPRi viability screens identify MIR17HG as a leading cell growth dependency in MM. (A) Schematic of CRISPRi viability screens. (B) Robust rank algorithm (RRA)-based ranked analysis of lncRNA dependencies in the secondary screen, considering 4 MM cell lines either together or individually. The top lncRNA dependency, *MIR17HG*, is highlighted, along with the protein-coding genes IRF4 and MYC used as positive controls. (C) CCK-8 proliferation assay of MM cell lines (AMO1, H929, KMS11, and KMS12BM) stably expressing KRAB-dCAS9 fusion protein and transduced with lentivectors to conditionally express anti-*MIR17HG* sgRNAs. CCK-8 assay was performed at indicated time points after exposure to doxycycline (0.5 μg/mL). Cell proliferation is calculated compared with parental cells infected with the empty sgRNA vector and exposed to doxycycline under the same conditions. (D) CCK-8 proliferation assay of MM cell lines (n = 11) transfected with 2 different ASOs targeting the *MIR17HG* pre-RNA or a nontargeting ASO (NC). ASOs were used at a concentration of 25 nM. Cell viability was measured 2 and 4 days after electroporation, and it is represented as % viability compared with cells transfected with NC-ASO. Data from 1 out of 3 independent experiments are shown in panel D. Data present mean ± standard deviation in panel D. *$P < .05$ by Student *t* test.

Downloaded from http://ashpublications.org/blood/article-pdf/141/4/391/2031172/blood_bld-2022-016892-main.pdf by guest on 30 June 2023

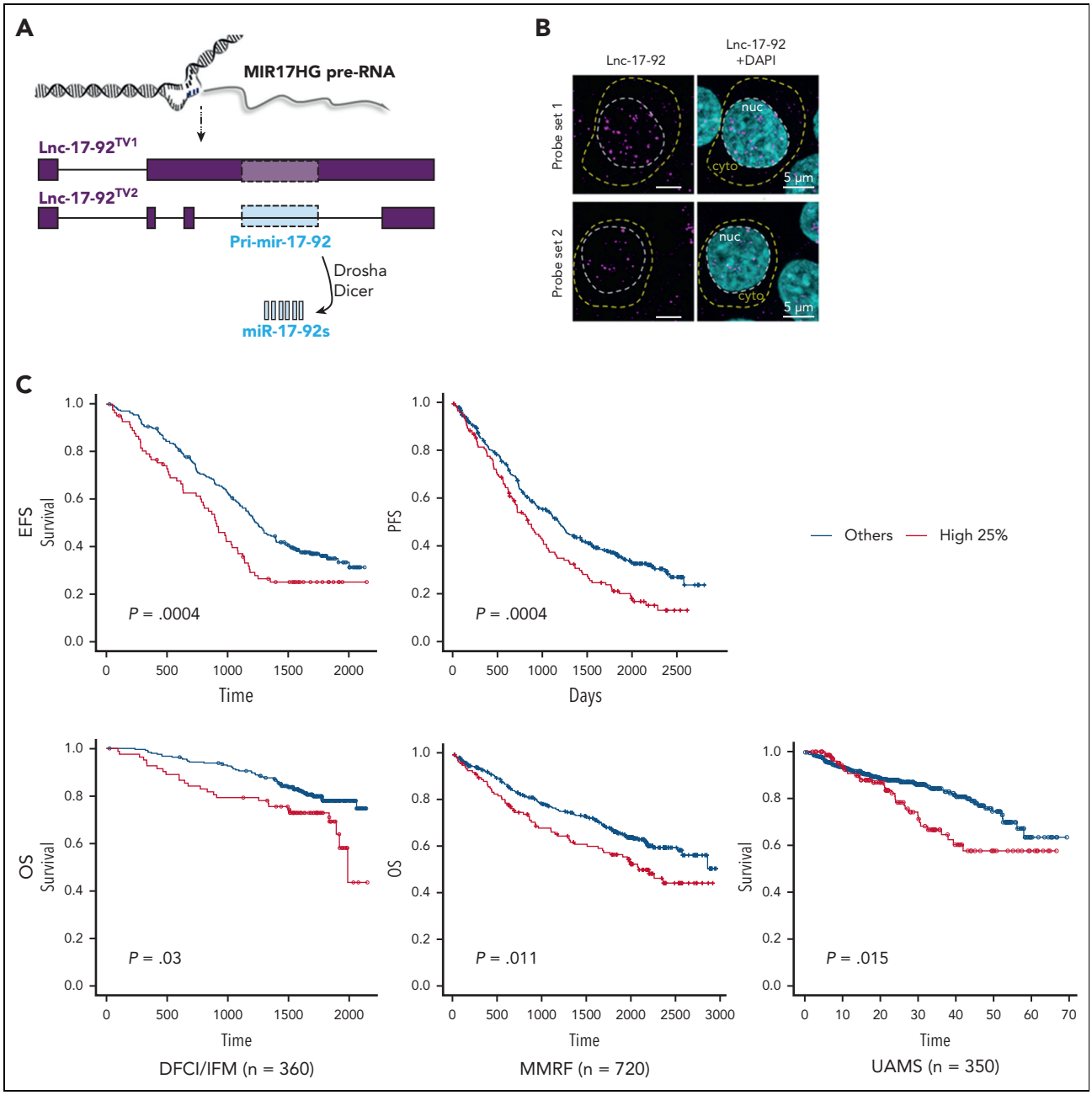

Figure 2. MIR17HG-derived lnc-17-92 mediates cell growth dependency in an miRNA- and DROSHA-independent manner. (A) Overview of *MIR17HG* locus, including both lncRNA (lnc-17-92)- and miRNA (miR-17-92)-derived transcripts. (B) Single molecule RNA FISH analysis of subcellular localization of lnc-17-92 in AMO1. Cell nuclei are stained by 4′,6-diamidino-2-phenylindole (DAPI). (C) Prognostic significance (event-free survival [PFS] and overall survival [OS]) of high lnc-17-92 expression (top quartile) in 3 large cohorts of MM patients. (D) CCK-8 proliferation assay in AMO1 and H929 cells stably transduced with either a lentivector carrying pri-mir-17-92 (pri-miR) or a lentiviral vector carrying GFP as a control and transfected with 2 different ASOs targeting the 5′ end (5′-ASO) of MIR17HG pre-RNA or a scrambled control (NC). Effects on cell proliferation were assessed 48 hours after transfection. (E) CCK-8 proliferation assay of DROSHA WT or KO AMO1 and H929 exposed to ASO1 (1 μM for AMO1 and 2.5 μM for H929) for 6 days. Western blot analysis of DROSHA expression in WT and KO cells. Vinculin was used as a protein-loading control. (F) Effects of lnc-17-92 depletion in a matrigel-based AMO1$^{DR\text{-}KO}$ xenograft in NOD SCID mice. Tumor growth of AMO1$^{DR\text{-}KO}$ with (ASO-1) or without (NC) lnc-17-92 depletion. (G) Survival analysis of tumor-injected mice. *P < .05. ns, not significant (P > .05 after Student t test).

diagnosis and/or relapse (supplemental Figures 2F-G) and that higher expression of lnc-17-92 was associated with shorter event-free survival and overall survival in 3 large cohorts of newly diagnosed MM patients (Figure 2C). Expression of lnc-17-92 did not significantly correlate with the expression of miR-17-92 miRNAs in CD138^{+} MM cells from 140 patients (average Spearman r = 0.16), suggesting that lnc-17-92 and miR-17-92 are under independent regulatory control and function in distinct molecular pathways mediating cell growth dependency to *MIR17HG* (supplemental Figure 2H).

To test independent activity of lnc-17-92, we first established 2 MM cell lines overexpressing miR-17-92 via ectopic expression of the primary precursor pri-mir-17-92 (supplemental Figure 3A).

Downloaded from http://ashpublications.org/blood/article-pdf/141/4/391/2031172/blood_bld-2022-016892-main.pdf by guest on 30 June 2023

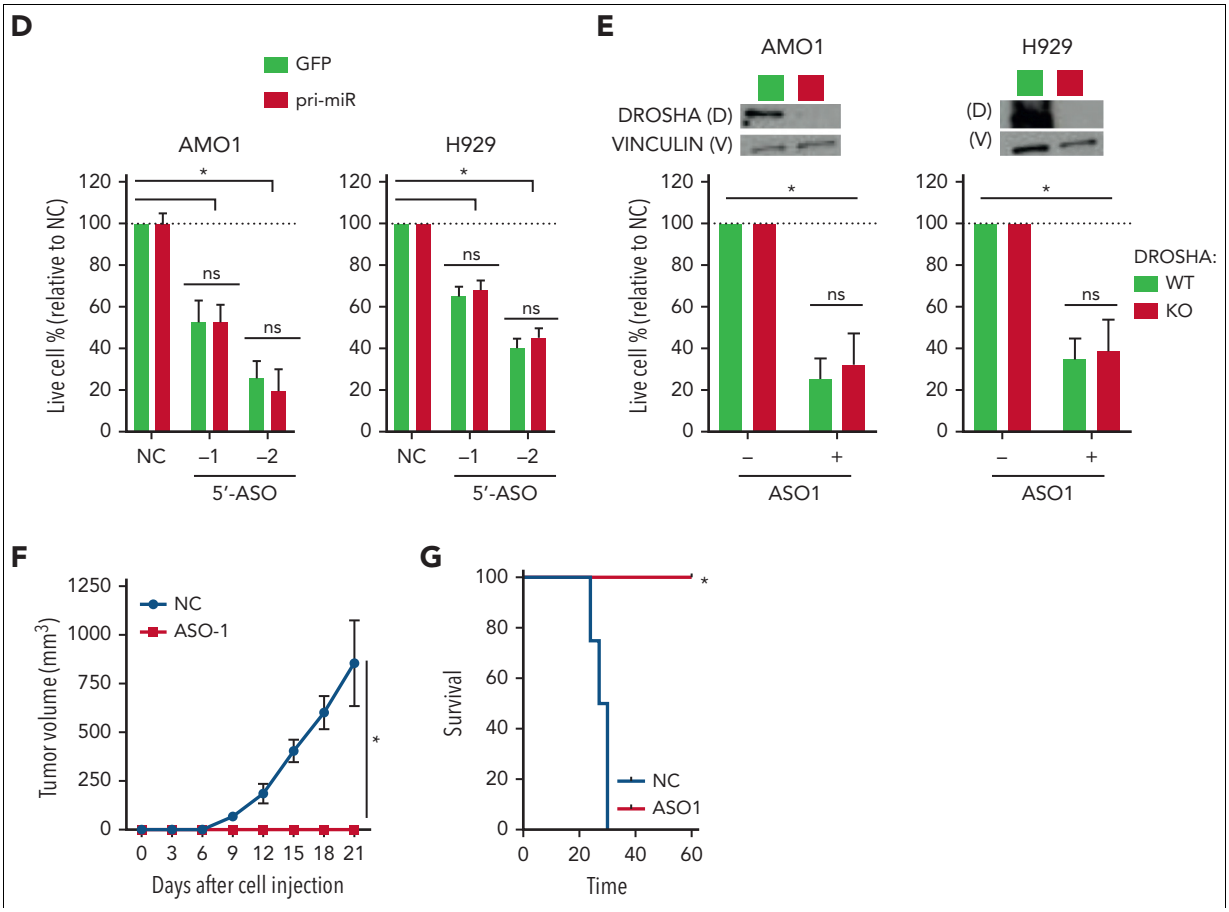

Figure 2 (continued)

We specifically depleted lnc-17-92 in these cell lines with ASOs targeting the 5′ end of MIR17HG pre-RNA, a region not covered by pri-mir-17-92, and observed a significant inhibition of cell growth that was not rescued by ectopic pri-mir-17-92 (Figure 2D). Next, we established 2 DROSHA knockout (DR-KO) MM cell lines (AMO1$^{DR\text{-}KO}$ and H929$^{DR\text{-}KO}$), which are unable to enzymatically digest pri-mir-17-92 and produce miR-17-92s (supplemental Figure 3B),[36] and still observed strong antiproliferative activity in both DR-WT and DR-KO cell systems after lnc-17-92 depletion using gymnotic treatment with ASO1 (Figure 2E) or after transfection with 3 different ASOs (−1/−2/−3) (supplemental Figure 3C). Importantly, exposure to gymnotic ASO1 (Figure 2E-F) or transfection with ASO2 (supplemental Figure 3D) abrogated the ability of AMO1$^{DR\text{-}KO}$ cells to establish tumors in nonobese diabetic severe combined immunodeficiency (NOD SCID) mice, resulting in prolonged animal survival. Next, using the easy-to-transfect colorectal cancer cell line HCT-116, which is driven by *MIR17HG*,[34] we found that ectopic expression of lnc-17-92^{TV1} significantly rescued the antiproliferative activity of ASOs targeting *MIR17HG* pre-RNA more effectively than ectopic lnc-17-92^{TV2} or pri-mir-17-92 (supplemental Figure 3E-F). Finally, we confirmed the independent activity of lnc-17-92 in the HCT-116 and DLD-1 colorectal cancer cell lines carrying a mutant Dicer, which confers a hypomorphic phenotype preventing the cells from enzymatically processing mature miRNAs[37] (supplemental Figure 3G).

These results indicate that lnc-17-92^{TV1} is the main mediator of *MIR17HG* cancer dependency, separate from the actions and biogenesis pathway of miR-17-92.

Lnc-17-92 forms a transcriptional axis with *ACACA* to promote MM cell growth

The nuclear enrichment of lnc-17-92 suggests a possible role in the regulation of gene expression. We therefore depleted lnc-17-92 in DR-WT (AMO1 and H929) and DR-KO (AMO1$^{DR\text{-}KO}$) MM cell lines using early exposure to gymnotic ASO1 to avoid modulation of miR-17-92 (supplemental Figure 4A) and miR-17-92's canonical targets in DROSHA WT cells (supplemental Figure 4B-C) and identified 7 genes rapidly downregulated after depletion of lnc-17-92 in all the cell lines tested (Figure 3A). We validated these findings in CD138^{+} cells from 3 MM patients treated ex vivo with ASO1 (Figure 3B) and in the lymphoma cell lines Raji and Daudi (supplemental Figure 4D). Conversely, the expression of these genes was not affected by modulating individual members of miR-17-92 using synthetic mimics or inhibitors (supplemental Figure 4E-F). Moreover, we observed significant positive correlation (Spearman $r > 0.3$; $P < .001$) between lnc-17-92 and its target genes in at least 1 out of 2 large RNA-seq MM patient data sets (IFM/DFCI and MMRF/CoMMpass) (Figure 3C).

Downloaded from http://ashpublications.org/blood/article-pdf/141/4/391/2031172/blood_bld-2022-016892-main.pdf by guest on 30 June 2023

Using a luciferase reporter assay, performed in 293T$^{DR\text{-}KO}$ cells in the presence or absence of lnc-17-92 depletion, we demonstrated that the regulatory control of lnc-17-92 over these genes, except *ANO6*, occurs at the promoter level (Figure 3D). Consistently, we confirmed lnc-17-92 interaction at the promoter region of the top target, *ACACA*, by a ChIRP assay followed by qRT-PCR analysis (Figure 3E; supplemental Figure 4G-H) and showed frequent localization of lnc-17-92 to the *ACACA* locus by single-molecule dual RNA FISH analysis of lnc-17-92 and *ACACA* pre-mRNA (<300 nm to nearest lnc-17-92 spot in ~50% of *ACACA* pre-RNA spots analyzed [n = 60]) (Figure 3F). Proximal localization of lnc-17-92 to the *ACACA* gene locus was significantly more frequent compared with random spots (Figure 3F).

Among the identified lnc-17-92 targets, *ACACA* had the largest impact on the proliferation and survival of MM cells (Figure 3G). *ACACA* encodes the rate-limiting enzyme for the de novo lipogenesis pathway ACC1, which supports tumorigenesis in different cancer contexts.[38] To confirm that lnc-17-92's control over *ACACA* expression has a functional effect, we depleted lnc-17-92 and found that the incorporation of C^{14}-radiolabeled glucose into the lipid pool was significantly reduced, indicating a reduced amount of de novo lipogenesis,[24] both in MM cell lines and CD138$^+$ MM patient cells (supplemental Figure 4I). This was not observed after transfection of MM cells with synthetic inhibitors of miR-17-92s (supplemental Figure 4J). Moreover, supplementing palmitate, which is the main downstream product of ACC1 activity, significantly rescued the antiproliferative and pro-apoptotic effects of lnc-17-92 depletion in MM cells (supplemental Figure 4K-L).

Altogether, these data indicate lnc-17-92 is a chromatin-interacting lncRNA with transcriptional regulatory functions. We next sought to determine how it can promote transcription by searching for its protein-binding partners.

Lnc-17-92 directly interacts with c-MYC and promotes its occupancy at the *ACACA* promoter

The targeting of *MIR17HG* primarily kills c-MYC–positive (MYC$^+$) tumor cells, including in MM.[5,34,39,40] Intriguingly, MYC is known to reactivate *ACACA* expression and de novo lipogenesis in tumor cells,[41] with MYC$^+$ tumor cells becoming addicted to this metabolic pathway, findings that we validated in MM cells (supplemental Figure 5A-D). Therefore, we hypothesized that lnc-17-92 mediates the functional interplay between MYC and *MIR17HG* by directly interacting with MYC protein to promote gene expression.

We performed an RNA protein pull-down (RPPD) experiment and found that MYC forms a complex with lnc-17-92^{TV1} (Figure 4A). RIP assay with MYC antibody confirmed the enrichment of lnc-17-92^{TV1} (Figure 4B). Moreover, an RNA yeast-3-hybrid (Y3H) assay confirmed the lnc-17-92^{TV1}–MYC interaction in an in vivo cellular model,[42] as shown by yeast colony growth (Figure 4C). An analysis using truncated versions of lnc-17-92^{TV1} further indicated the 3'-end regions, which do not include miR-17-92, as particularly relevant for the interaction with MYC in MM cells (supplemental Figure 5E).

Next, we evaluated whether MYC and lnc-17-92 cooperate to promote *ACACA* expression in MM cells. Depletion of lnc-17-92 in MM cells indeed abrogated MYC occupancy at the *ACACA* promoter while not affecting MYC expression (Figure 4D) and reduced the expression of *ACACA* in the conditional MYC Tet-Off cell line P493-6[43] only in presence of high MYC levels (Figure 4E). Moreover, by coupling RNA FISH analysis of lnc-17-92^{TV1} and *ACACA* pre-RNA with immunofluorescence analysis of MYC protein, we captured the colocalization of lnc-17-92^{TV1} and MYC at the *ACACA* gene locus (supplemental Figure 5F).

These data demonstrate that lnc-17-92^{TV1} forms an RNA-protein complex with the transcription factor MYC to promote its chromatin occupancy and transcriptional activity at the *ACACA* promoter.

Lnc-17-92 mediates the assembly of an MYC-WDR82 transcriptional complex, leading to transcriptional and epigenetic activation of *ACACA*

MYC transcriptional activity is modulated through the interaction with transcriptional and epigenetic coregulators.[41] To determine whether lnc-17-92 affects these protein-protein interactions, we integrated the results of a proximity-dependent BioID analysis (supplemental Figure 6A) with a Co-IP/MS in 3 MM cell lines (AMO1, H929, and U266^{MYC+}), in the presence and absence of depletion of lnc-17-92. This analysis highlighted WDR82 as a very high-confidence lnc-17-92–dependent MYC interactor (Figure 5A and supplemental Tables 4-7). A direct RNA-protein interaction between lnc-17-92^{TV1} and WDR82 was further confirmed by both RPPD (Figure 5B) and RNA Y3H (Figure 5C) assays. Analysis using the truncated versions of lnc-17-92^{TV1} indicated that this interaction may involve different domains across lnc-17-92 (supplemental Figure 6B).

WDR82 is a regulatory component of the SET1 methyltransferase complex, which catalyzes histone H3 Lys-4 (H3K4) methylation (mono-, di-, tri-) at the transcriptional start sites of active loci,[44,45] a prerequisite for MYC binding to chromatin and transactivation.[46] We confirmed a global effect of silencing of WDR82 on H3K4 methylation in MM cells (supplemental Figure 6C). Consistently, depletion of WDR82 reduced the occupancy of H3K4me3 (Figure 5D and supplemental Figure 6D) and MYC (Figure 5E and supplemental Figure 6E) at the *ACACA* promoter and decreased *ACACA* mRNA expression (Figure 5F and supplemental Figure 6F) in MM cells. Furthermore, using MM cells expressing an ectopic WDR82-GFP fusion protein (supplemental Figure 6G), we demonstrated that lnc-17-92 expression is essential for WDR82 occupancy at the *ACACA* promoter (Figure 5G). Additionally, lnc-17-92 depletion resulted in reduced levels of H3K4me3 at the *ACACA* promoter (Figure 5H), without globally impacting the H3K4 methylation status (Figure 5I).

These findings suggest lnc-17-92^{TV1} is a chromatin scaffold mediating the assembly of the MYC-WDR82 multiprotein transcriptional complex to control the expression of *ACACA* and likely other genes.

Downloaded from http://ashpublications.org/blood/article-pdf/141/4/391/2031172/blood_bld-2022-016892-main.pdf by guest on 30 June 2023

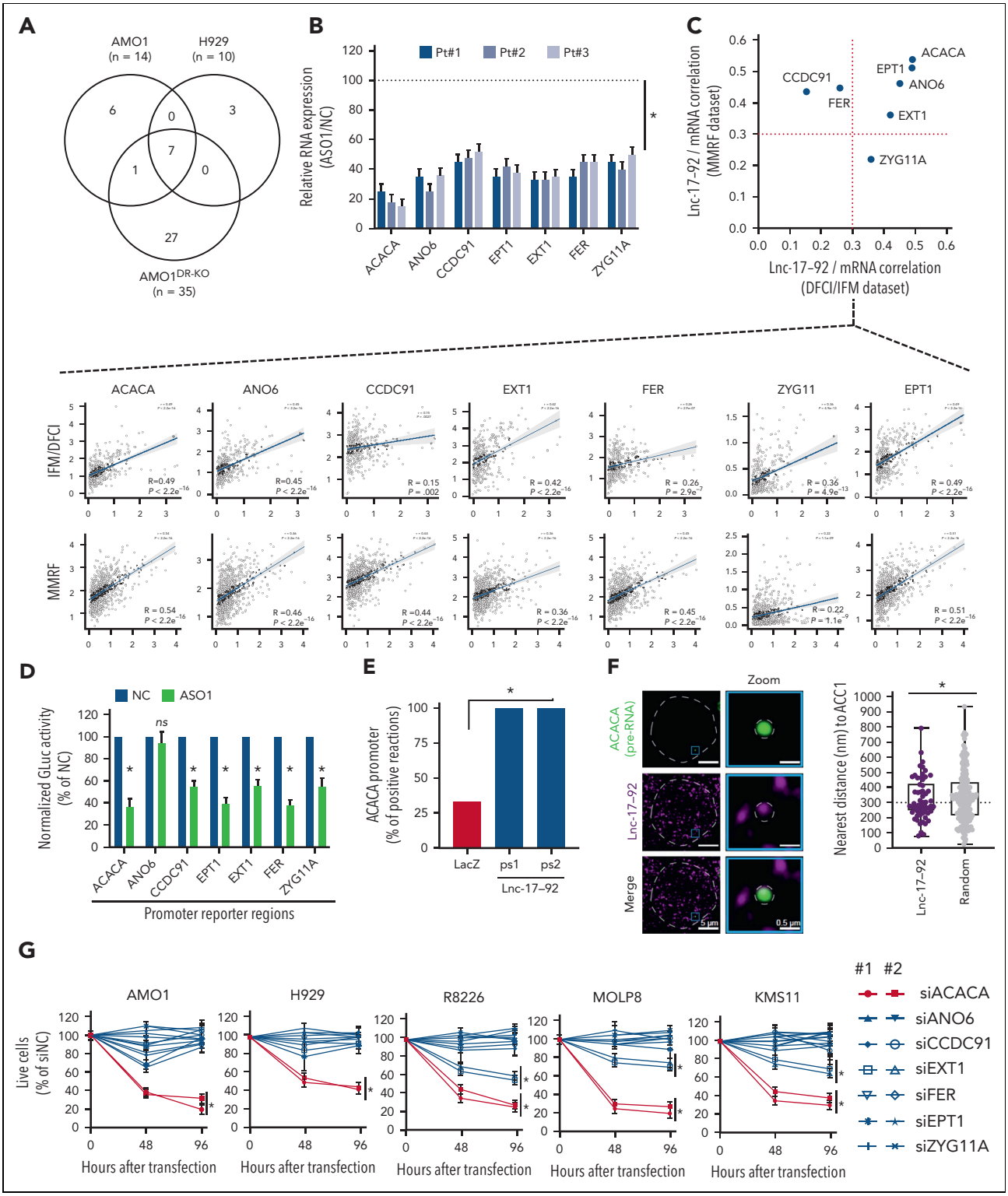

Figure 3. Lnc-17-92 forms a transcriptional axis with *ACACA* to promote proliferation and survival of MM cells. (A) Transcriptomic analysis after lnc-17-92 depletion in MM cell lines that have either DROSHA WT (AMO1, H929) or KO (AMO1^{DR-KO}). Venn diagram of commonly downregulated genes (adjusted $P < .05$; log2FC < −1). Cells were exposed to ASO1 for 24 hours. (B) qRT-PCR analysis of lnc-17-92 targets in CD138^{+} cells from 3 MM patients exposed to ASO1 for 24 hours. The results shown are average mRNA expression levels after normalization with GAPDH and ΔΔCt calculations. RNA level in cells exposed to NC (vehicle) were set as an internal reference. (C) Correlation analysis between lnc-17-92 targets (mRNA) and lnc-17-92 in CD138^{+} MM patient cells from 2 large RNA-seq cohorts (DFCI/IFM, n = 360; MMRF/CoMMpass, n = 720). Spearman *r* obtained in DFCI/IFM (x-axis) and MMRF/CoMMpass (y-axis) data sets. Dotted red lines indicate $r = 0.3$. Individual correlation plots (below). (D) GLuc/SEAP dual reporter assay showing reduced activity of *ACACA*, *ANO6*, *CCDC91*, *EPT1*, *EXT1*, *FER*, and *KIAA1109* promoter activity after lnc-17-92 knockdown using ASO1. The reporter vectors were cotransfected into 293T cells with either ASO1 or control ASO. Cells were harvested for the luciferase activity assay 48 hour after transfection. Results are shown as % of normalized GLuc activity in ASO1-transfected cells compared with control. (E) ChIRP-qPCR analysis showing effective amplification of *ACACA* promoter in chromatin purified using 2 lnc-17-92 antisense probe sets (ps1 and ps2), compared with chromatin purified using LacZ antisense probes (negative control). (F) (left) Snapshot obtained by

Downloaded from http://ashpublications.org/blood/article-pdf/141/4/391/2031172/blood_bld-2022-016892-main.pdf by guest on 30 June 2023

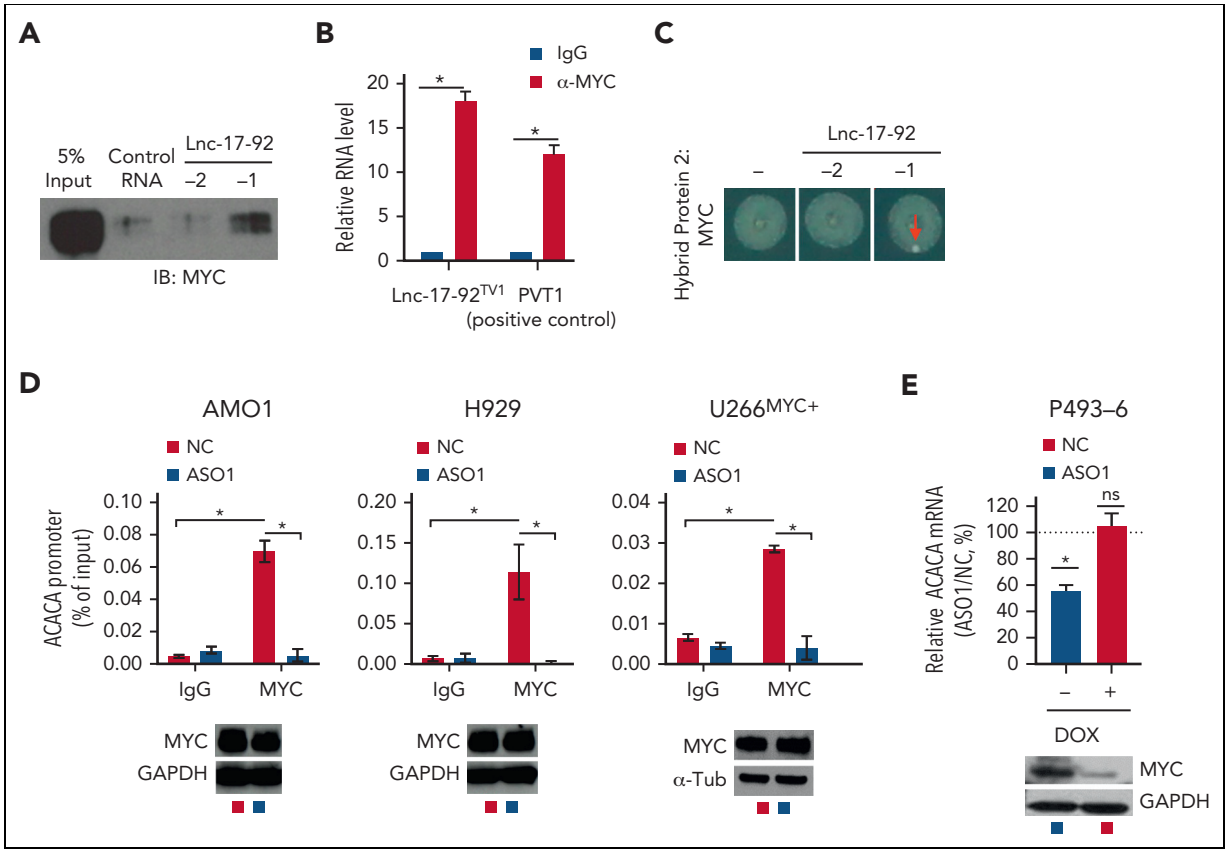

Figure 4. Lnc-17-92 directly interacts with c-MYC and promotes its occupancy at the *ACACA* promoter. (A) Western blot analysis of MYC in RPPD material precipitated with control RNA or lnc-17-92^{TV1} or lnc-17-92^{TV2}. 5% input is used as a reference. (B) qRT-PCR analysis of lnc-17-92 (detecting lnc-17-92^{TV1}) in RIP material precipitated using an anti-MYC antibody (α-MYC) or immunoglobulin G (IgG) control. LncRNA PVT1 is used as a positive control for its role as MYC interactor. (C) RNA Y3H using MYC as hybrid protein 2 and, as hybrid RNAs, a negative control RNA (–) or lnc-17-92^{TV1} or lnc-17-92^{TV2}. (D) ChIP-qPCR analysis of MYC occupancy at the *ACACA* promoter in AMO1, H929, and U266^{MYC+} exposed for 24 hours to ASO1 or NC (vehicle). MYC occupancy at *ACACA* promoter is calculated as % of input chromatin. Western blot analysis of MYC from paired samples (below). GAPDH or α-tubulin were used as protein loading controls. (E) qRT-PCR analysis of *ACACA* mRNA in P493-6 cells exposed for 2 days to either doxycycline or DMSO to knock down MYC and then exposed for 2 additional days to either ASO1 or vehicle (NC) to deplete lnc-17-92. *ACACA* expression levels in cells exposed to NC were set as an internal reference. *$P < .05$, Student *t* test.

Therapeutic inhibitors of *MIR17HG* exert potent antitumor activity in vitro and in vivo in animal models of human MM

We next explored MIR17HG as a therapeutic target, which includes both the lncRNA and miRNA factors. To develop clinically applicable inhibitors, we screened >80 fully phosphorothioated, 2′-O-methoxyethyl–modified, lipid-conjugated ASOs that could either trigger RNase H–mediated degradation of MIR17HG pre-RNA (gapmeRs) or exert function via an RNase H–independent mechanism (blockmeRs)[47] (supplemental Figure 7A-B). This procedure identified an 18-mer tocopherol (T)-conjugated gapmeR G2-15b-T ("G") and an 18-mer tocopherol (T)-conjugated steric blocker SB9-19-T ("B") as both having strong antiproliferative effects (cell growth inhibition >50%) in a large panel of MM cell lines as well as CD138$^+$ primary MM cells, while sparing (cell growth inhibition <50%) nonmalignant cell lines (THLE-2, HK-2, HS-5, and 293T) and peripheral blood mononuclear cells from 3 healthy donors (supplemental Figure 7C).

To assess the in vivo antitumor activity of both compounds, we first used an AMO1-based plasmacytoma xenograft model in immunocompromised NOD SCID mice. Here, we observed a significant reduction of tumor growth after a treatment cycle with either G2-15b-T (tumor growth inhibition [TGI] = 76%) or B9-19-T (TGI = 69%) (Figure 6A). Analysis of tumors retrieved from mice following this treatment confirmed reduced expression of lnc-17-92 (Figure 6B) and miR-17-92s (supplemental Figure 7D), as well as modulation of lnc-17-92's targets (*ACACA*, *EPT1*, *EXT1*, *CCDC91*, *ANO6*, *FER*, and *ZYG11A*) (Figure 6C) and miR-17-92's target BIM (also known as *BCL2L11*) (supplemental Figure 7E). We also observed reduced levels of tripalmitin (supplemental Figure 7F), a surrogate for the de novo lipogenesis product palmitate[48] This demonstrates efficient uptake of G2-15b-T and B9-19-T by tumor cells in vivo. We observed no overt toxicity in the mice after treatment, as shown by blood cell count, clinical biochemistry (supplemental Tables 9-10), and body weight analysis (not shown).

Figure 3 (continued) dual RNA-FISH analysis of *ACACA* pre-mRNA (green) and lnc-17-92 (purple) in a representative AMO1 cell; (right) box plot showing the distance (nm) of *ACACA* pre-RNA spots to the nearest lnc-17-92 spots (n = 57) or to the nearest random spots (160); 300 nm was used as a cut-off determining proximity. (G) CCK-8 proliferation assay in 5 MM cells lines after transfection with siRNAs against lnc-17-92 targets. Two siRNAs were used for each target, plus a scramble siRNA (NC) as a control. Cell viability was measured at the indicated time point, represented as % of NC-transfected cells. *$P < .05$ after Student *t* test in panels B, D, and G or after Fisher exact test in panels E and F. Pt, patient.

Downloaded from http://ashpublications.org/blood/article-pdf/141/4/391/2031172/blood_bld-2022-016892-main.pdf by guest on 30 June 2023

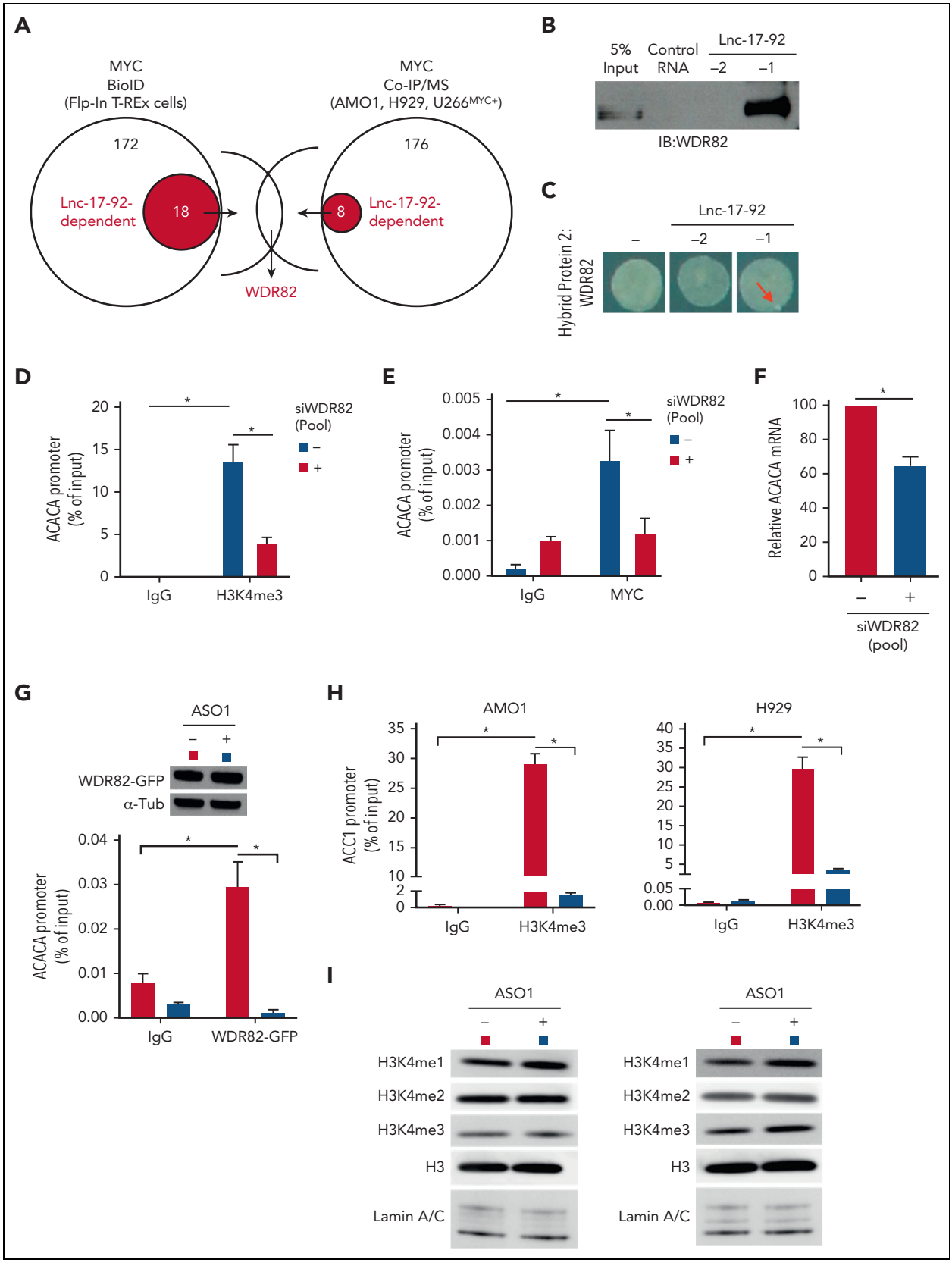

Figure 5. Lnc-17-92 mediates the assembly of a MYC-WDR82 transcriptional complex, leading to transcriptional and epigenetic activation of *ACACA*. (A) Schematic of integrated BioID and coimmunoprecipitation assay followed by mass-spectrometry analysis (Co-IP/MS) assays to explore the MYC-protein interacting network in the presence or absence of lnc-17-92 depletion. (B) Western blot analysis of WDR82 in RPPD material precipitated with lnc-17-92^{TV1} or lnc-17-92^{TV2} or with control RNA; 5% input is used as a reference. (C) RNA Y3H using WDR82 as hybrid protein 2 and, as hybrid RNAs, either a negative control RNA (–) or lnc-17-92^{TV1} or lnc-17-92^{TV2}. Red arrows indicate yeast colony growth. (D) ChIP-qPCR analysis of H3K4me3 occupancy at *ACACA* promoter after silencing of WDR82 with a siRNA pool (n-4) in H929 (24-hour time point). Data are

Downloaded from http://ashpublications.org/blood/article-pdf/141/4/391/2031172/blood_bld-2022-016892-main.pdf by guest on 30 June 2023

We next confirmed the significant anti-MM activity of G2-15b-T and B9-19-T in an aggressive model of diffused myeloma, in which tumor growth of MOLP8-luc$^+$ MM cells is assessed by BLI. In this model, tumor growth was significantly antagonized after a treatment cycle with either G2-15b-T (TGI = 84%) or B9-19-T (TGI = 52%). Treatment with G2-15b-T resulted in tumor clearance in 2 out of 8 mice (25%) (Figure 6D). Importantly, both inhibitors significantly prolonged animal survival (Figure 6E).

Finally, we established a clinically relevant PDX-NSG mouse model by tail-vein injection of CD138$^+$ MM cells obtained from an advanced-stage patient (PDX-NSG). In this model, tumor growth was monitored in serum samples using human κ light chain as a surrogate. Remarkably, we observed a regression of tumor growth after a treatment cycle with G2-15b-T, whose effects were comparable to bortezomib (a positive control) (Figure 6F).

Discussion

MIR17HG is often amplified and/or overexpressed in human cancer and has a driver role.[34,39,49] One of its transcriptional products, pri-mir-17-92, is enzymatically digested by DROSHA into 6 precursor transcripts (pre-mir-17/−18a/−19a/−20a/−19b1/−92a) that are further processed by DICER to generate the miR-17-92 mature miRNAs (miR-17/−18a/−19a/−20a/−19b1/−92a). These miRNAs posttranscriptionally repress relevant tumor-suppressive mRNAs,[34,39,40,49] such as the pro-apoptotic factor BIM.[50] Their impact on tumorigenesis is particularly relevant when coexpressed with MYC,[34,39] as there is a well-documented interplay between miR-17-92, especially miR-19b,[51,52] and MYC transcriptional targets in maintaining cancer cell homeostasis.[5,39,40] We have previously demonstrated that these miRNAs play a relevant role in MM by forming homeostatic feed-forward loops with MYC and BIM.[5] Interestingly, our previous work also showed that depletion of mature miRNAs does not phenocopy the inhibition of *MIR17HG* pre-RNA, suggesting other tumor-promoting functions for this transcript.[5] An alternative mechanism to explain the oncogenic role of *MIR17HG* has been recently identified and involves the overload of DROSHA by an overexpressed pri-mir-17-92 in B-cell lymphomas.[53] Our description in this study of the miRNA-, DROSHA-, and DICER-independent function of *MIR17HG*, via lnc-17-92, establishes this gene as having both *short* (miR-17-92) and *long* (lnc-17-92) noncoding RNA activities, with the latter mediating tumor-promoting activity in MM and likely other cancer contexts (eg, colorectal cancer).

We described lnc-17-92 as a specific regulator of gene expression via chromatin occupancy and interaction with MYC and WDR82. Lnc-17-92 directly reduces the expression of a small subset of genes and prevents the accumulation of H3K4me3 at the *ACACA* promoter. These effects are in contrast to what is observed by depleting c-MYC (ie, global effect on gene expression) or WDR82 (ie, global effect on methylation of H3K4) in cancer cells, as reported in this and other studies.[44,54] Our data support the emerging paradigm whereby chromatin occupancy by transcription factors like MYC may be determined through interacting with specific lncRNAs,[55] in addition to protein partners.[26] In a broader perspective, our observations on lnc-17-92 suggest lncRNAs are key mediators of the epigenetic and transcriptional reprogramming of MM cells. In this molecular scenario, whereas proteins act as catalytic effectors, the intrinsic structural flexibility of lncRNAs makes them good modular scaffolds able to mediate both protein-protein and protein-DNA interactions at specific chromatin regions.

We further showed that the lnc-17-92–MYC–WDR82 complex impacts tumor cell metabolism by activating the de novo lipogenesis pathway via regulation of *ACACA*. This anabolic pathway is primarily restricted to liver and adipose tissue in normal adults but is reactivated in cancer cells via mechanisms yet to be fully described.[38,56] Notably, MYC has been implicated in the reprogramming of tumor-cell metabolism by activating that pathway via *ACACA* and other genes.[57] In turn, lipogenesis has emerged as an essential pathway for the onset and progression of MYC-driven cancers, which are susceptible to pharmacologic inhibition of ACC1.[41] This seems particularly relevant in MM, in which tumor cells need to adapt their metabolic pathways to meet the high bioenergetic and biosynthetic demand posed by the malignant cell growth coupled with unceasing production of monoclonal immunoglobulin.[58,59] Nevertheless, we acknowledge that the oncogenic roles of lnc-17-92 are likely not limited to the transcriptional axis with *ACACA* and will require further investigation to be comprehensively elucidated.

Deletion of MIR17HG is tolerated in adult mice,[60] and its haploinsufficiency is compatible with life in humans.[61] The physiological role of MIR17HG seems particularly relevant only for the hematopoietic stem cell compartment,[60] which continuously renews. These observations support the development of *MIR17HG* as a target. Thus, for translational purposes, we developed 2 therapeutic ASOs that target the *MIR17HG* pre-RNA via different mechanisms of action (ie, RNase H–dependent or –independent). With the recent advances in RNA medicine,[62-64] the use of ASOs to therapeutically antagonize disease-driver genes is becoming increasing possible,[47,65] including in MM therapy.[5,66] Our optimization of design and chemistry has helped to overcome the major obstacles to the clinical use of ASOs, such as poor bioavailability,[65] while limiting off-target toxicity. The inhibitors described here bear state-of-the-art chemical modifications (2′MOE, phosphorothioated-backbone, lipid conjugation) and have sufficient nucleotide length (18 mer) to ensure high specificity for *MIR17HG*. Inhibitors of this kind have already been tested within clinical trials, and a few are already approved by the US Food and

Figure 5 (continued) represented as % of input chromatin. (E) ChIP-qPCR analysis of MYC occupancy at the *ACACA* promoter after silencing of WDR82 with a siRNA pool (n-4) (24-hour time point). Data are represented as % of input chromatin. (F) qRT-PCR analysis of *ACACA* mRNA after silencing of WDR82 with a siRNA pool (n-4) (48-hour time point). Raw Ct values were normalized to GAPDH mRNA and expressed as ΔΔCt values calculated using the comparative cross threshold method. *ACACA* expression levels in cells transfected with NC were set as an internal reference. (G) ChIP-qPCR analysis of WDR82-GFP occupancy at the *ACACA* promoter in AMO1 exposed for 24 hours to gymnotic ASO1. Data are represented as % of input chromatin. Western blot analysis of WDR82-GFP from paired samples. α-Tubulin was used as the protein loading control. (H) ChIP-qPCR analysis of H3K4me3 occupancy at the *ACACA* promoter in AMO1 and H929 exposed for 24 hours to gymnotic ASO1. Data are represented as % of input chromatin. (I) Western blot analysis of H3, H3H3K4me1, H3H3K4me2, and H3H3K4me3 in AMO1 and H929 exposed for 24 hours to gymnotic ASO1. Lamin A/C was used as the protein loading controls (nuclear lysates). *$P < .05$, Student *t* test.

Downloaded from http://ashpublications.org/blood/article-pdf/141/4/391/2031172/blood_bld-2022-016892-main.pdf by guest on 30 June 2023

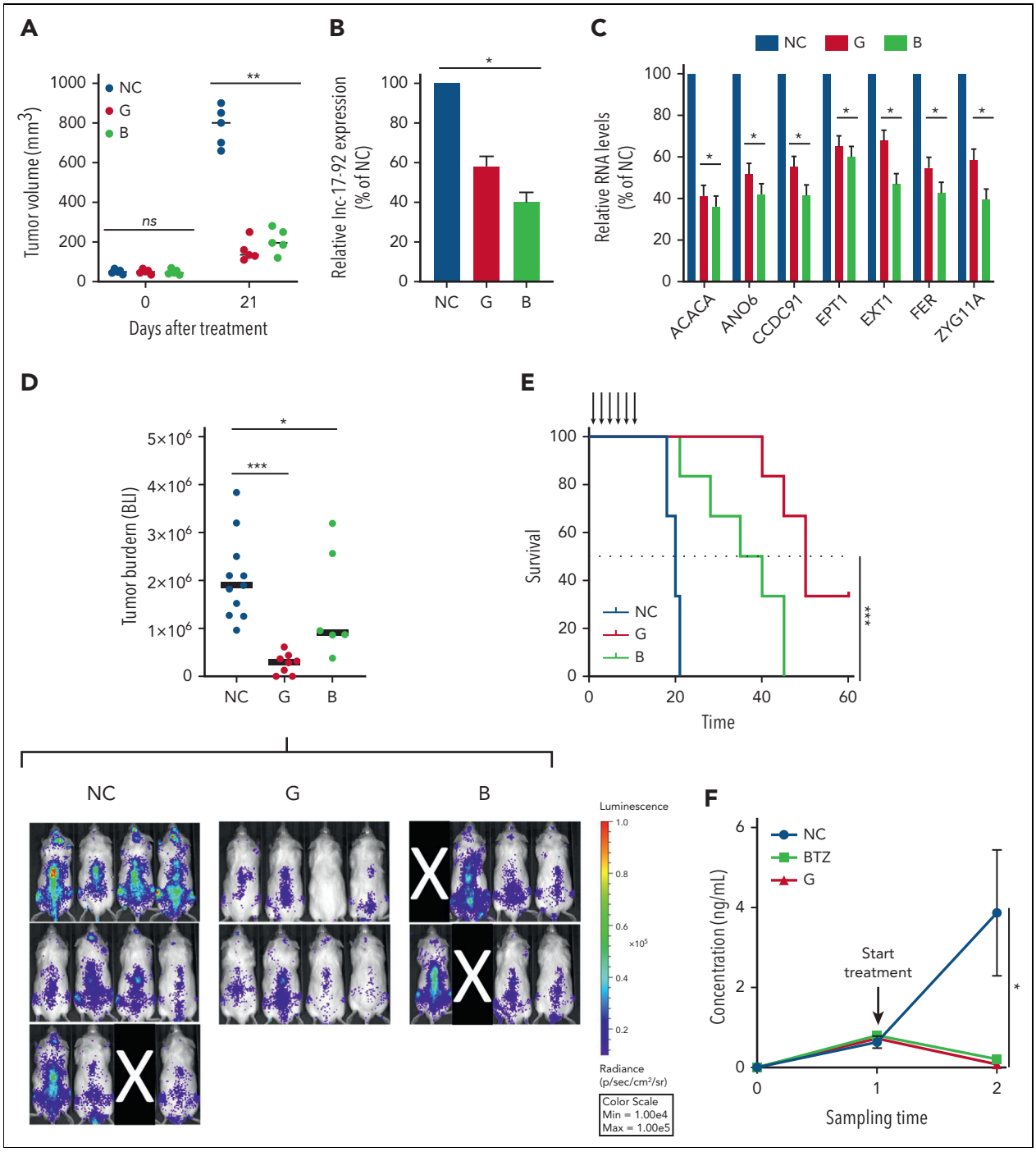

Figure 6. Therapeutic inhibitors of MIR17HG exert potent antitumor activity in vitro and in vivo in animal models of human MM. (A) Subcutaneous in vivo tumor growth of AMO1 cells in NOD SCID mice, 21 days after treatment with G2-15b*-TO (G; n = 5), B9-19-TO (B; n = 5), or vehicle (NC; n = 5). (B-C) qRT-PCR analysis of lnc-17-92 (C) and lnc-17-92 targets (D) in AMO1 xenografts, retrieved from animals treated with G2-15b*-TO (G; n = 1), B9-19-TO (B; n = 1), or vehicle (NC; n = 1) as a control. Raw Ct values were normalized to *ACTB* mRNA and expressed as ΔΔCt values calculated using the comparative cross threshold method. Expression levels in NC were set as an internal reference. (D) Bioluminescent imaging–based (BLI-based) measurement of in vivo tumor growth of MOLP8-luc^{+} in NSG mice, after treatment with G2-15b*-TO (G; n = 8), B9-19-TO (B; n = 6), or vehicle (NC; n = 11). On the top, a scatter plot shows the analysis of bioluminescence intensity. Red bars indicate median value. Bioluminescence was measured at the end of the treatment cycle (day 15). Image acquisition (below). Mice removed from the study owing to failed IV injection of tumor cells are covered by a black rectangle. (E) Survival analysis from experiment in panel E. (F) Human κ light chain enzyme-linked immunosorbent assay–based measurement of in vivo tumor growth of MM patient cells in NSG mice (PDX-NSG), after treatment with G2-15b*-TO (G; n = 2), bortezomib (BTZ; n = 2), or vehicle (NC; n = 3). Black arrows indicate treatments. *P < .05; **P < .01; ***P < .001. Max, maximum; Min, minimum; ns, not significant.

Drug Administration for use in different human diseases.[65] Our optimized ASOs targeting *MIR17HG* with demonstrated activity in 3 different murine models of human MM provide the rationale to now consider clinical application in MM.

Different questions remain open about the dual nature of *MIR17HG* and its therapeutic targeting. Important future directions will be to uncover how the splicing of *MIR17HG* is alternatively regulated to produce lnc-17-92 or miR-17-92 and

Downloaded from http://ashpublications.org/blood/article-pdf/141/4/391/2031172/blood_bld-2022-016892-main.pdf by guest on 30 June 2023

to address the relative contribution of lnc-17-92 and miR-17-92 to the oncogenic activity of *MIR17HG* in other cancer models. Whether the host genes of the 2 paralogs of miR-17-92, miR-106a-363 and miR-25-106b, also retain miRNA-independent function will be an important line of investigation.

Overall, this study establishes *MIR17HG* with a unique lncRNA function of facilitating protein-protein and protein-DNA interactions, mediating tumor-promoting activity with therapeutic implications.

Acknowledgments

The authors gratefully acknowledge the members of their laboratories for technical advice and critical discussions. The authors thank Christina Usher (Dana-Farber Cancer Institute) for editing the manuscript and insightful comments;Dirk Eick (Helmholtz-Zentrum München, Molecular Epigenetics), Christoph Driessen (Cantonal Hospital St Gallen, St Gallen, Switzerland), and Linda Penn (Princess Margaret Cancer Centre, University Health Network, Toronto, Ontario, Canada) for providing the relevant cellular models; Pierosandro Tagliaferri (Magna Graecia University, Catanzaro, Italy) for insightful discussions on the dual long and short nature of *MIR17HG*; Benjamin Izar and Johannes Melms (Columbia University, New York, NY) for insightful discussions on CRISPR viability screen methodology; and the "8th Annual Miracles for Myeloma 5K Virtual Run/Walk" organizers and attendees for the fundraising in support to this research project.

This work is supported by NIH/NCI grants SPORE-P50CA100707, R01-CA050947, R01CA207237, P01CA155258, R01-CA178264 (N.C.M., K.C.A.); by VA Healthcare System grant No. 5I01BX001584 (N.C.M.); by the Paula and Roger Riney Foundation grant (N.C.M. and K.C.A.); by NIH/NCI grants RO1CA131945, R01CA187918, P50 CA211024 and Department of Defense grants DoD PC160357 and DoD PC180582 (M.L.); by the Sheldon and Miriam Medical Research Foundation (K.C.A.); by the Italian Association for Cancer Research (AIRC) with "Special Program for Molecular Clinical Oncology–5 per mille," 2010/15 and its Extension Program No. 9980, 2016/18 (P.T.). E.M. is supported by a Brian D. Novis Junior Grant from the International Myeloma Foundation, by a Career Enhancement Award from Dana Farber/Harvard Cancer Center SPORE in Multiple Myeloma (SPORE-P50CA100707), by a Special Fellow grant from The Leukemia & Lymphoma Society, and by a Scholar Award from the American Society of Hematology. A.G. is supported by a Fellow grant from The Leukemia & Lymphoma Society and by a Scholar Award from the American Society of Hematology. J.E.H. is supported by a NIH F32 fellowship (NCI 1F32CA254216-01). A.N. is supported by a grant from the Italian Association for Cancer Research (AIRC, IG24365). N.A. is supported by a grant from the Italian Association for Cancer Research (AIRC, IG24449). K.C.A. is an American Cancer Society Clinical Research Professor.

Authorship

Contribution: E.M. and N.C.M. conceived and designed the research studies; E.M., M.F., and N.C.M. wrote the manuscript; M.K.S., A.A.-S., and K.T. performed in silico analysis of transcriptomic data; C.F.R. performed lipidomic studies; L.W.-L. performed yeast-3-hybrid experiments; J.E.H. performed RNA FISH, dual RNA FISH, and Co-IF/dual RNA FISH; S.T. generated MM cells expressing Cas9; W.D.P. analyzed ChIP-seq data; S.G. designed t-ASOs; C.F., N.A.R., D.M., and F.S. provided support for the identification of lnc-17-92 isoforms; M.F., A.G., D.G., N.L., D.M., N.A., M.J., G.B., C.L., Y.-T.T., A.N., D.C., T.H., M.A.S., P.T., R.A.Y., K.C.A., C.D.N., and M.L. contributed to the design and interpretation of key experiments; M.L. supervised lipidomic studies; and C.D.N. supervised Y3H experiments.

Conflict-of-interest disclosure: N.C.M. serves on advisory boards of and as consultant to Takeda, BMS, Celgene, Janssen, Amgen, AbbVie, Oncopep, Karyopharm, Adaptive Biotechnology, and Novartis and holds equity ownership in Oncopep. K.C.A. serves on advisory boards to Janssen, Pfizer, Astrazeneca, Amgen, Precision Biosciences, Mana, Starton, and Raqia and is a Scientific Founder of OncoPep and C4 Therapeutics. R.A.Y. is a founder and shareholder of Syros Pharmaceuticals, Camp4 Therapeutics, Omega Therapeutics, and Dewpoint Therapeutics. E.M., S.G., and N.C.M filed a provisional patent on *MIR17HG* as a target for cancer therapy. D.C. reports other support from Stemline Therapeutics, Oncopeptides, and C4 Therapeutics outside the submitted work. The remaining authors declare no competing financial interests.

ORCID profiles: E.M., 0000-0002-8850-0442; C.F.R., 0000-0002-6785-6933; J.E.H., 0000-0002-9604-2007; A.A.-S., 0000-0002-0183-0562; W.D.P., 0000-0002-4069-4954; G.B., 0000-0003-3673-0104; N.A.R., 0000-0001-5773-0803; C.L., 0000-0002-9155-090X; A.N., 0000-0001-9047-5912; M.A.S., 0000-0002-8932-6829; R.A.Y., 0000-0001-8855-8647.

Correspondence: Nikhil C. Munshi, Dana-Farber Cancer Institute, Jerome Lipper Myeloma Center, Harvard Medical School, 450 Brookline Ave., Boston, MA 02215; email: nikhil_munshi@dfci.harvard.edu; and Eugenio Morelli, Dana-Farber Cancer Institute, Jerome Lipper Myeloma Center, Harvard Medical School, 450 Brookline Ave., Boston, MA 02215; email: eugenio_morelli@dfci.harvard.edu.

Footnotes

Submitted 2 May 2022; accepted 13 September 2022; prepublished online on *Blood* First Edition 20 September 2022. https://doi.org/10.1182/blood.2022016892.

Data reported in this article have been deposited in the General Expression Omnibus database (accession number GSE208599).

The authors declare that all data supporting the findings of this study are available within the article and its supplemental information. Files or reagents are available from the corresponding authors, Nikhil C. Munshi and Eugenio Morelli (nikihil_munchi@dfci.harvard.edu and eugenio_morelli@dfci.harvard.edu) on request.

The online version of this article contains a data supplement.

There is a *Blood* Commentary on this article in this issue.

The publication costs of this article were defrayed in part by page charge payment. Therefore, and solely to indicate this fact, this article is hereby marked "advertisement" in accordance with 18 USC section 1734.

REFERENCES

1. Gulla A, Anderson KC. Multiple myeloma: the (r)evolution of current therapy and a glance into future. *Haematologica*. 2020;105(10):2358-2367.
2. Morelli E, Gulla A, Rocca R, et al. The non-coding RNA landscape of plasma cell dyscrasias. *Cancers (Basel)*. 2020;12(2):320.
3. Pichiorri F, Suh SS, Rocci A, et al. Downregulation of p53-inducible microRNAs 192, 194, and 215 impairs the p53/MDM2 autoregulatory loop in multiple myeloma development. *Cancer Cell*. 2016;30(2):349-351.
4. Amodio N, Stamato MA, Juli G, et al. Drugging the lncRNA MALAT1 via LNA gapmeR ASO inhibits gene expression of proteasome subunits and triggers anti-multiple myeloma activity. *Leukemia*. 2018;32(9):1948-1957.
5. Morelli E, Biamonte L, Federico C, et al. Therapeutic vulnerability of multiple myeloma to MIR17PTi, a first-in-class inhibitor of pri-miR-17-92. *Blood*. 2018;132(10):1050-1063.
6. Hu Y, Lin J, Fang H, et al. Targeting the MALAT1/PARP1/LIG3 complex induces DNA damage and apoptosis in multiple myeloma. *Leukemia*. 2018;32(10):2250-2262.
7. Morelli E, Leone E, Cantafio ME, et al. Selective targeting of IRF4 by synthetic microRNA-125b-5p mimics induces

Downloaded from http://ashpublications.org/blood/article-pdf/141/4/391/2031172/blood_bld-2022-016892-main.pdf by guest on 30 June 2023

anti-multiple myeloma activity in vitro and in vivo. *Leukemia*. 2015;29(11):2173-2183.

8. Leone E, Morelli E, Di Martino MT, et al. Targeting miR-21 inhibits in vitro and in vivo multiple myeloma cell growth. *Clin Cancer Res*. 2013;19(8):2096-2106.

9. Wang Z, Yang B, Zhang M, et al. lncRNA epigenetic landscape analysis identifies EPIC1 as an oncogenic lncRNA that interacts with MYC and promotes cell-cycle progression in cancer. *Cancer Cell*. 2018; 33(4):706-720.e9.

10. Hon CC, Ramilowski JA, Harshbarger J, et al. An atlas of human long non-coding RNAs with accurate 5′ ends. *Nature*. 2017; 543(7644):199-204.

11. Ulitsky I, Bartel DP. LncRNAs: genomics, evolution, and mechanisms. *Cell*. 2013; 154(1):26-46.

12. Lu Y, Zhao X, Liu Q, et al. LncRNA MIR100HG-derived miR-100 and miR-125b mediate cetuximab resistance via Wnt/beta-catenin signaling. *Nat Med*. 2017;23(11): 1331-1341.

13. Tseng YY, Moriarity BS, Gong W, et al. PVT1 dependence in cancer with MYC copy-number increase. *Nature*. 2014;512(7512):82-86.

14. Gutschner T, Diederichs S. The hallmarks of cancer: a long non-coding RNA point of view. *RNA Biol*. 2012;9(6):703-719.

15. Samur MK, Minvielle S, Gulla A, et al. Long intergenic non-coding RNAs have an independent impact on survival in multiple myeloma. *Leukemia*. 2018;32(12):2626-2635.

16. Carrasco-Leon A, Ezponda T, Meydan C, et al. Characterization of complete lncRNAs transcriptome reveals the functional and clinical impact of lncRNAs in multiple myeloma. *Leukemia*. 2021;35(5):1438-1450.

17. Ronchetti D, Agnelli L, Taiana E, et al. Distinct lncRNA transcriptional fingerprints characterize progressive stages of multiple myeloma. *Oncotarget*. 2016;7(12):14814-14830.

18. Liu SJ, Horlbeck MA, Cho SW, et al. CRISPRi-based genome-scale identification of functional long noncoding RNA loci in human cells. *Science*. 2017;355(6320):aah7111.

19. Morelli E, et al. CRISPR interference (CRISPRi) and CRISPR activation (CRISPRa) to explore the oncogenic lncRNA network. In: Navarro A, eds. *Long Non-Coding RNAs in Cancer. Methods in Molecular Biology*. Vol 2348. New York, NY: Humana; 2021. https://doi.org/10.1007/978-1-0716-1581-2_13

20. Taiana E, et al. In vitro silencing of lncRNAs using LNA gapmeRs. In: Navarro A, eds. *Long Non-Coding RNAs in Cancer. Methods in Molecular Biology*. Vol 2348. New York, NY: Humana; 2021. https://doi.org/10.1007/978-1-0716-1581-2_10

21. Shaffer SM, Wu MT, Levesque MJ, Raj A. Turbo FISH: a method for rapid single molecule RNA FISH. *PLoS One*. 2013;8(9):e75120.

22. Raj A, van den Bogaard P, Rifkin SA, van Oudenaarden A, Tyagi S. Imaging individual mRNA molecules using multiple singly labeled probes. *Nat Methods*. 2008;5(10):877-879.

23. Chu C, Quinn J, Chang HY. Chromatin isolation by RNA purification (ChIRP). *J Vis Exp*. 2012;61:e3912.

24. Zadra G, Ribeiro CF, Chetta P, et al. Inhibition of de novo lipogenesis targets androgen receptor signaling in castration-resistant prostate cancer. *Proc Natl Acad Sci U S A*. 2019;116(2):631-640.

25. Fulciniti M, Lin CY, Samur MK, et al. Non-overlapping control of transcriptome by promoter- and super-enhancer-associated dependencies in multiple myeloma. *Cell Rep*. 2018;25(13):3693-3705.e6.

26. Kalkat M, Resetca D, Lourenco C, et al. MYC protein interactome profiling reveals functionally distinct regions that cooperate to drive tumorigenesis. *Mol Cell*. 2018;72(5): 836-848.e7.

27. Li W, Xu H, Xiao T, et al. MAGeCK enables robust identification of essential genes from genome-scale CRISPR/Cas9 knockout screens. *Genome Biol*. 2014;15(12):554.

28. Shaffer AL, Emre NC, Lamy L, et al. IRF4 addiction in multiple myeloma. *Nature*. 2008; 454(7201):226-231.

29. Chesi M, Robbiani DF, Sebag M, et al. AID-dependent activation of a MYC transgene induces multiple myeloma in a conditional mouse model of post-germinal center malignancies. *Cancer Cell*. 2008;13(2): 167-180.

30. Jovanovic KK, Escure G, Demonchy J, et al. Deregulation and targeting of TP53 pathway in multiple myeloma. *Front Oncol*. 2018;8:665.

31. Tessoulin B, Moreau-Aubry A, Descamps G, et al. Whole-exon sequencing of human myeloma cell lines shows mutations related to myeloma patients at relapse with major hits in the DNA regulation and repair pathways. *J Hematol Oncol*. 2018;11(1):137.

32. Lai F, Damle SS, Ling KK, Rigo F. Directed RNase H cleavage of nascent transcripts causes transcription termination. *Mol Cell*. 2020;77(5):1032-1043.e4.

33. Lee JS, Mendell JT. Antisense-mediated transcript knockdown triggers premature transcription termination. *Mol Cell*. 2020; 77(5):1044-1054.e3.

34. He L, Thomson JM, Hemann MT, et al. A microRNA polycistron as a potential human oncogene. *Nature*. 2005;435(7043):828-833.

35. Ota A, Tagawa H, Karnan S, et al. Identification and characterization of a novel gene, C13orf25, as a target for 13q31-q32 amplification in malignant lymphoma. *Cancer Res*. 2004;64(9):3087-3095.

36. Bartel DP. MicroRNAs: genomics, biogenesis, mechanism, and function. *Cell*. 2004;116(2): 281-297.

37. Cummins JM, He Y, Leary RJ, et al. The colorectal microRNAome. *Proc Natl Acad Sci U S A*. 2006;103(10):3687-3692.

38. Rohrig F, Schulze A. The multifaceted roles of fatty acid synthesis in cancer. *Nat Rev Cancer*. 2016;16(11):732-749.

39. Li Y, Choi PS, Casey SC, Dill DL, Felsher DW. MYC through miR-17-92 suppresses specific target genes to maintain survival, autonomous proliferation, and a neoplastic state. *Cancer Cell*. 2014;26(2):262-272.

40. Izreig S, Samborska B, Johnson RM, et al. The miR-17 approximately 92 microRNA cluster is a global regulator of tumor metabolism. *Cell Rep*. 2016;16(7):1915-1928.

41. Gouw AM, Margulis K, Liu NS, et al. The MYC oncogene cooperates with sterol-regulated element-binding protein to regulate lipogenesis essential for neoplastic growth. *Cell Metab*. 2019;30(3):556-572.e5.

42. Hook B, Bernstein D, Zhang B, Wickens M. RNA-protein interactions in the yeast three-hybrid system: affinity, sensitivity, and enhanced library screening. *RNA*. 2005;11(2): 227-233.

43. Schuhmacher M, Staege MS, Pajic A, et al. Control of cell growth by c-Myc in the absence of cell division. *Curr Biol*. 1999;9(21): 1255-1258.

44. Lee JH, Skalnik DG. Wdr82 is a C-terminal domain-binding protein that recruits the Setd1A histone H3-Lys4 methyltransferase complex to transcription start sites of transcribed human genes. *Mol Cell Biol*. 2008;28(2):609-618.

45. Beurton F, Stempor P, Caron M, et al. Physical and functional interaction between SET1/COMPASS complex component CFP-1 and a Sin3S HDAC complex in C. elegans. *Nucleic Acids Res*. 2019;47(21):11164-11180.

46. Amente S, Lania L, Majello B. Epigenetic reprogramming of Myc target genes. *Am J Cancer Res*. 2011;1(3):413-418.

47. Puttaraju M, Jackson M, Klein S, et al. Systematic screening identifies therapeutic antisense oligonucleotides for Hutchinson-Gilford progeria syndrome. *Nat Med*. 2021; 27:526-535.

48. Falchook G, Infante J, Arkenau HT, et al. First-in-human study of the safety, pharmacokinetics, and pharmacodynamics of first-in-class fatty acid synthase inhibitor TVB-2640 alone and with a taxane in advanced tumors. *EClinicalMedicine*. 2021;34: 100797.

49. Mogilyansky E, Rigoutsos I. The miR-17/92 cluster: a comprehensive update on its genomics, genetics, functions and increasingly important and numerous roles in health and disease. *Cell Death Differ*. 2013; 20(12):1603-1614.

50. Labi V, Peng S, Klironomos F, et al. Context-specific regulation of cell survival by a miRNA-controlled BIM rheostat. *Genes Dev*. 2019;33(23-24):1673-1687.

51. Olive V, Bennett MJ, Walker JC, et al. miR-19 is a key oncogenic component of mir-17-92. *Genes Dev*. 2009;23(24):2839-2849.

52. Olive V, Sabio E, Bennett MJ, et al. A component of the mir-17-92 polycistronic oncomir promotes oncogene-dependent apoptosis. *Elife*. 2013;2:e00822.

Downloaded from http://ashpublications.org/blood/article-pdf/141/4/391/2031172/blood_bld-2022-016892-main.pdf by guest on 30 June 2023

53. Donayo AO, Johnson RM, Tseng HW, et al. Oncogenic biogenesis of pri-miR-17 approximately 92 reveals hierarchy and competition among polycistronic microRNAs. *Mol Cell*. 2019;75(2):340-356.e10.

54. Lin CY, Loven J, Rahl PB, et al. Transcriptional amplification in tumor cells with elevated c-Myc. *Cell*. 2012;151(1):56-67.

55. Zhang B, Lu HY, Xia YH, Jiang AG, Lv YX. Long non-coding RNA EPIC1 promotes human lung cancer cell growth. *Biochem Biophys Res Commun*. 2018;503(3):1342-1348.

56. Beloribi-Djefaflia S, Vasseur S, Guillaumond F. Lipid metabolic reprogramming in cancer cells. *Oncogenesis*. 2016;5:e189.

57. Stine ZE, Walton ZE, Altman BJ, Hsieh AL, Dang CV. MYC, metabolism, and cancer. *Cancer Discov*. 2015;5(10):1024-1039.

58. Masarwi M, DeSchiffart A, Ham J, Reagan MR. Multiple myeloma and fatty acid metabolism. *JBMR Plus*. 2019;3(3):e10173.

59. El Arfani C, De Veirman K, Maes K, De Bruyne E, Menu E. Metabolic features of multiple myeloma. *Int J Mol Sci*. 2018;19(4):1200.

60. Brinkmann K, Ng AP, de Graaf CA, et al. miR17~92 restrains pro-apoptotic BIM to ensure survival of haematopoietic stem and progenitor cells. *Cell Death Differ*. 2020;27(5):1475-1488.

61. Sirchia F, Di Gregorio E, Restagno G, et al. A case of Feingold type 2 syndrome associated with keratoconus refines keratoconus type 7 locus on chromosome 13q. *Eur J Med Genet*. 2017;60(4):224-227.

62. Sullenger BA, Nair S. From the RNA world to the clinic. *Science*. 2016;352(6292):1417-1420.

63. Crooke ST, Witztum JL, Bennett CF, Baker BF. RNA-targeted therapeutics. *Cell Metabol*. 2018;27(4):714-739.

64. Damase TR, Sukhovershin R, Boada C, Taraballi F, Pettigrew RI, Cooke JP. The limitless future of RNA therapeutics. *Front Bioeng Biotechnol*. 2021;9:628137.

65. Dhuri K, Bechtold C, Quijano E, et al. Antisense oligonucleotides: an emerging area in drug discovery and development. *J Clin Med*. 2020;9(6):2004.

66. Mondala PK, Vora AA, Zhou T, et al. Selective antisense oligonucleotide inhibition of human IRF4 prevents malignant myeloma regeneration via cell cycle disruption. *Cell Stem Cell*. 2021;28(4):623-636.e9.

© 2023 by The American Society of Hematology

Downloaded from http://ashpublications.org/blood/article-pdf/141/4/391/2031172/blood_bld-2022-016892-main.pdf by guest on 30 June 2023